THEORETICAL ANALYSIS ON ACOUSTIC FIELDS FORMED BY FOCUSING DEVICES IN ACOUSTIC MICROSCOPY

Y. SUGAWARA, J. KUSHIBIKI, and N. CHUBACHI
Department of Electrical Engineering
Faculty of Engineering
Tohoku University
Sendai 980, Japan

ABSTRACT

Equations have been derived to discuss the convergent field distributions formed by the three different focusing devices, such as an acoustic lens, a concave transducer and an off-centric concave transducer, which are practically employed in acoustic microscopy. The field distribution near the focusing area can be systematically investigated by introducing two parameters D and E, where $D=a^2/R_L \lambda_L$ (a; the radius of concave aperture, R_L; the radius of curvature of concave aperture, and λ_L; the wavelength in the liquid couplant) and $E=(k_S/k_L)(\epsilon/(1+\epsilon))$ (k_S and k_L; the propagation constants in the solid rod and in the liquid couplant, respectively, and ϵ; the normalized eccentricity introduced for the systematical treatment of those focusing devices), respectively. The fields obtained by the present analysis are compared with those obtained by the direct calculation on the diffraction theory to reveal the validity of the present study. It is shown that the excellent focusing characteristics are expected with increasing of D and/or decreasing of E among the three focusing devices, which can be hardly speculated by the diffraction theory.

1. INTRODUCTION

A highly convergent acoustic beam in acoustic microscopy has been practically obtained by focusing devices such as an acoustic lens [1], a concave transducer [2] and/or an off-centric con-

cave transducer [3] as shown in Fig. 1. The total performance of the acoustic microscope strongly depends on the focusing characteristics of the focusing device being employed. So far, the focusing performance of each device has been investigated individually [4-12], so that unified analysis on the focusing devices is expected to discuss the relationship of the characteristics among them.

In this paper, the acoustic fields formed by these devices are theoretically investigated in order to obtain general understanding on the relationship in the focusing performance, so that two parameters, D and E, which dominate the convergent field distributions formed by these devices, have been derived. Further, taking a fused quartz and a sapphire as the solid rod materials, the field distributions obtained by the present approach are compared to those obtained by the numerical calculation under diffraction theory [11], where the diffraction of the acoustic fields in the solid rod and the transmittance for the acoustic waves propagating from the solid rod into the liquid couplant are taken into account, to reveal the significant advantage of the present approach for understanding the focusing characteristics.

2. THEORETICAL ANALYSIS

On the basis of an idea that the convergent field distribution is mainly affected by the phase distribution rather than the amplitude distribution
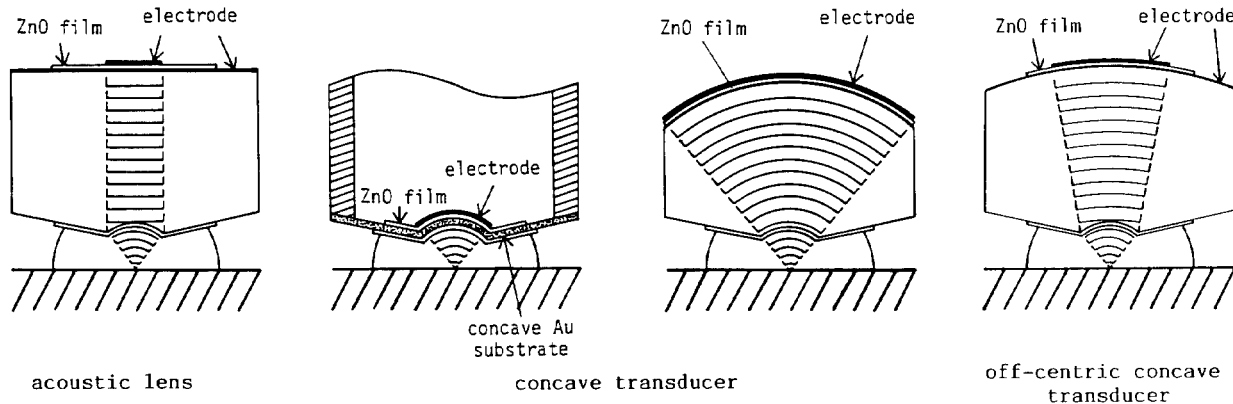

Fig. 1 Focusing devices in acoustic microscopy.

of acoustic waves on the concave surface facing to the liquid couplant, a theory is developed by combining two approaches: namely, wavefront optics and wave optics. First, by the wavefront optics approach, the field distribution on the concave surface is derived for each device to have uniform amplitude with the phase delay depending on the opening angle of the concave aperture. Next, by the wave optics approach, the field distribution near the focusing area formed by that on the concave aperture is derived using the Lommel's approximation method [13].

Figure 2 shows the geometrical configuration of the typical focusing device and a related coordinate system for calculation of the acoustic field. In Fig. 2, S denotes the spherical boundary between the solid rod and the liquid couplant, viz., the concave aperture. We define the rectangular coordinate system, (x,y,z), with the center of concave surface S as the origin O and the symmetric axis of the device as the z axis. Points C_1 and C_2 are the centers of curvature for the concave aperture and the concave transducer, respectively, fabricated on the solid rod. R_L is the radius of curvature of the concave aperture. The distance between C_1 and C_2 is given as εR_L, where ε is the normalized eccentricity defined as $\varepsilon = C_1 C_2 / R_L$ [12]. In Fig. 2, the off-centric concave transducer is representatively shown as the focusing device, because the acoustic lens and the concave transducer can be equivalent to the limiting cases of the normalized eccentricity, $\varepsilon = 0$ and $\varepsilon = \infty$, respectively, of the off-centric concave transducer. k_S and k_L are the propagation constants in the solid rod and the liquid, respectively.

Acoustic waves generated from the concave transducer on the solid rod propagate toward its center of curvature C_2 and arrive at the concave aperture S, and then is focused by the focusing function of acoustic lens. Now let us denote the field distribution radiated from S into the liquid as u_L. Then the field u_2 at the observation point p in the liquid can be obtained from the Rayleigh-Sommerfeld diffraction integral as follows:

$$u_2 = \frac{1}{j\lambda_L} \int_S u_L \frac{\exp(jk_L r_{12})}{r_{12}} ds_1 \qquad (1)$$

where ds_1 is the surface element on S, r_{12} is the distance between ds_1 and p. Here the obliquity factor is readily approximated by unity, and the time dependence $e^{-j\omega t}$ is omitted for simplicity.

Initially, let us consider the field distribution u_L. Referring to Fig. 2, let us take the coordinates (x_1,y_1,z_1) at an arbitrary point s on S. Further, we take the spherical coordinates (ρ,θ) such that $\rho^2 = x_1^2 + y_1^2 + z_1^2$, $\rho_h = x_1^2 + y_1^2$, $x_1 = \rho_h \cos\theta$, $y_1 = \rho_h \sin\theta$, where ρ is the chord between the origin O and the point s on S. From the concept of the wavefront optics, we assume that the field distribution $u_L(x_1,y_1,z_1)$ at the point s has the phase delay corresponding to the distance qs as
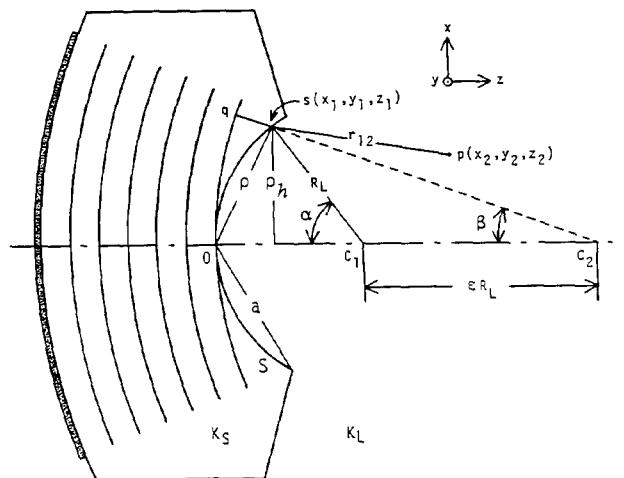

Fig. 2 Cross-sectional geometry of focusing device and the coordinate system used for analysis.

compared with the field $u_L(0,0,0)$ at the origin O. The distance qs can be now obtained as

$$qs = R_L[1+\varepsilon-\{(1+\varepsilon)^2-\varepsilon\rho^2/R_L^2\}^{1/2}] \qquad (2)$$

If $(1+\varepsilon)^2$ is much larger than the other terms, the distance qs can be approximated by

$$qs = \frac{1}{2R_L} \frac{\varepsilon}{1+\varepsilon} \rho^2 \qquad (3)$$

Therefore, the field distribution u_L can be expressed as

$$u_L = u_0\, e^{jk_S \frac{1}{2R_L} \frac{\varepsilon}{1+\varepsilon} \rho^2} \qquad (4)$$

where u_0 is the constant amplitude factor on S. Now u_0 is taken as unity. In Eq. (4), the phase delay increases in proportion to k_S and ρ^2. It also depends on the normalized eccentricity ε.

Next, let us consider the acoustic field u_2 at the observation point p in the liquid. It is sufficient to discuss the field on the x-z plane, because the focusing devices are symmetric with respect to the z axis. So, let the coordinates at the point p be $(x_2,0,z_2)$. In the same way as the derivation of the distance qs, the distance r_{12} between the surface element ds_1 and the point p can be approximated as

$$r_{12} = z_2 + \frac{x_2^2}{2z_2} - \frac{\rho_h x_2}{z_2}\cos\theta + \frac{R_L-z_2}{2R_L z_2}\rho^2 \qquad (5)$$

The surface element ds_1 on S is given by

$$ds_1 = \rho d\rho d\theta \qquad (6)$$

Substituting Eqs. (4), (5) and (6) into Eq. (1), the field u_2 can be expressed as

$$u_2(x_2,0,z_2) = \frac{k_L}{jz_2} e^{jk_L(z_2+\frac{x_2^2}{2z_2})}$$

$$\times \int_0^a e^{j(k_S\frac{\epsilon}{1+\epsilon}+k_L\frac{R_L-z_2}{z_2})\frac{\rho^2}{2R_L}} \rho J_0(-k_L\rho_h x_2/z_2)d\rho \quad (7)$$

where a is the radius of the concave aperture, and J_0 is a Bessel function of the first kind, zero order. By applying the integration of parts with Eq. (7),

$$u_2(x_2,0,z_2) = e^{jk_L\left[z_2+\frac{x_2^2}{2z_2}-\frac{1}{1-\frac{z_2}{R_L}(1-\frac{k_S}{k_L}\frac{\epsilon}{1+\epsilon})}\right]}$$

$$\times \frac{1}{1-\frac{z_2}{R_L}(1-\frac{k_S}{k_L}\frac{\epsilon}{1+\epsilon})}[1-e^{jY\frac{1+X^2}{2X}}\sum_{n=0}^{\infty}(-j)^n X^n J_n(Y)] \quad |X| \leq 1$$

or $\qquad\qquad\qquad\qquad\qquad\qquad\qquad\qquad (8)$

$$u_2(x_2,0,z_2) = e^{jk_L\left[z_2+\frac{x_2^2}{2z_2}+\frac{R_L}{2z_2}\{1-\frac{z_2}{R_L}(1-\frac{k_S}{k_L}\frac{\epsilon}{1+\epsilon})a^2\}\right]}$$

$$\times \frac{1}{1-\frac{z_2}{R_L}(1-\frac{k_S}{k_L}\frac{\epsilon}{1+\epsilon})}\sum_{n=1}^{\infty}(-j)^n(1/X)^n J_n(Y) \quad |X| \geq 1$$

where

$$X = \frac{1}{1-\frac{z_2}{R_L}(1-\frac{k_S}{k_L}\frac{\epsilon}{1+\epsilon})}\frac{x_2}{a} \quad , \quad Y = \frac{k_L a x_2}{z_2}$$

Further, by introducing the variables defined with the following equations

$$V = \frac{x_2}{a}, \quad W = \frac{z_2}{R_L}, \quad D = \frac{a^2}{R_L\lambda_L}, \quad E = \frac{k_S}{k_L}\frac{\epsilon}{1+\epsilon} \quad (9)$$

the variables in Eq. (8) can be replaced as follows:

$$\frac{1}{1-\frac{z_2}{R_L}(1-\frac{k_S}{k_L}\frac{\epsilon}{1+\epsilon})} = \frac{1}{1-W(1-E)}$$

$$\qquad\qquad\qquad\qquad\qquad\qquad\qquad (10)$$

$$X = \frac{V}{1-W(1-E)}$$

$$Y = \frac{2\pi DV}{W}$$

Therefore, the acoustic fields on the (V,W) plane can be determined only by the parameters D and E. Here, the parameters V and W are the relative distances normalized by a and R_L, respectively. On the other hand, the parameter D, depending on a, R_L and λ_L, is the normalized depth of the concave aperture S. The parameter E, depending on k_S, k_L and ϵ, is the velocity ratio multiplied the normalized eccentricity ϵ.

The focal point giving the greatest amplitude on the z axis is obtained by

$$z_2 = \frac{R_L}{1-\frac{k_S}{k_L}\frac{\epsilon}{1+\epsilon}}[1-\frac{3}{\{\frac{k_L a^2}{4R_L}(1-\frac{k_S}{k_L}\frac{\epsilon}{1+\epsilon})\}^2-6}] \quad (11)$$

Equation (11) shows that the focal point is on the concave aperture side of the paraxial focal point given by the equation that $z_2=R_L/[1-(k_S/k_L)(\epsilon/(1+\epsilon))]$, and approaches it with increasing D.

3. CALCULATED RESULTS

According to the theoretical analysis of the focused acoustic fields developed above, numerical calculations are carried out taking fused quartz and sapphire as materials of solid rod. The focusing characteristics obtained by the present theory are compared with those by the direct calculation under the diffraction theory [11] to reveal the validity of the present study.

Figure 3 shows the acoustic field distributions along the z axis and at the focal plane calculated for a fused quartz rod. The parameters are as follows: the acoustic frequency is 200 MHz, and the radius of curvature of the concave aperture is 1.0 mm. Figure 3 shows the acoustic fields for three cases; (a) D=135 and E=0.2 (ϵ=4.0, α_m=60°), (b) D=135 and E=0.25 ($\epsilon=\infty$, α_m=60°), and (c) D=63 and E=0.2 (ϵ=4.0, α_m=45°), where α_m is the maximum opening angle of the concave aperture. As easily seen from the figures, the values of the normalized eccentricity ϵ and the opening angle α_m are closely related to the focusing characteristics. As the parameter E increases, the focal length becomes longer. As the parameter D decreases, the width of mainlobe becomes wider.
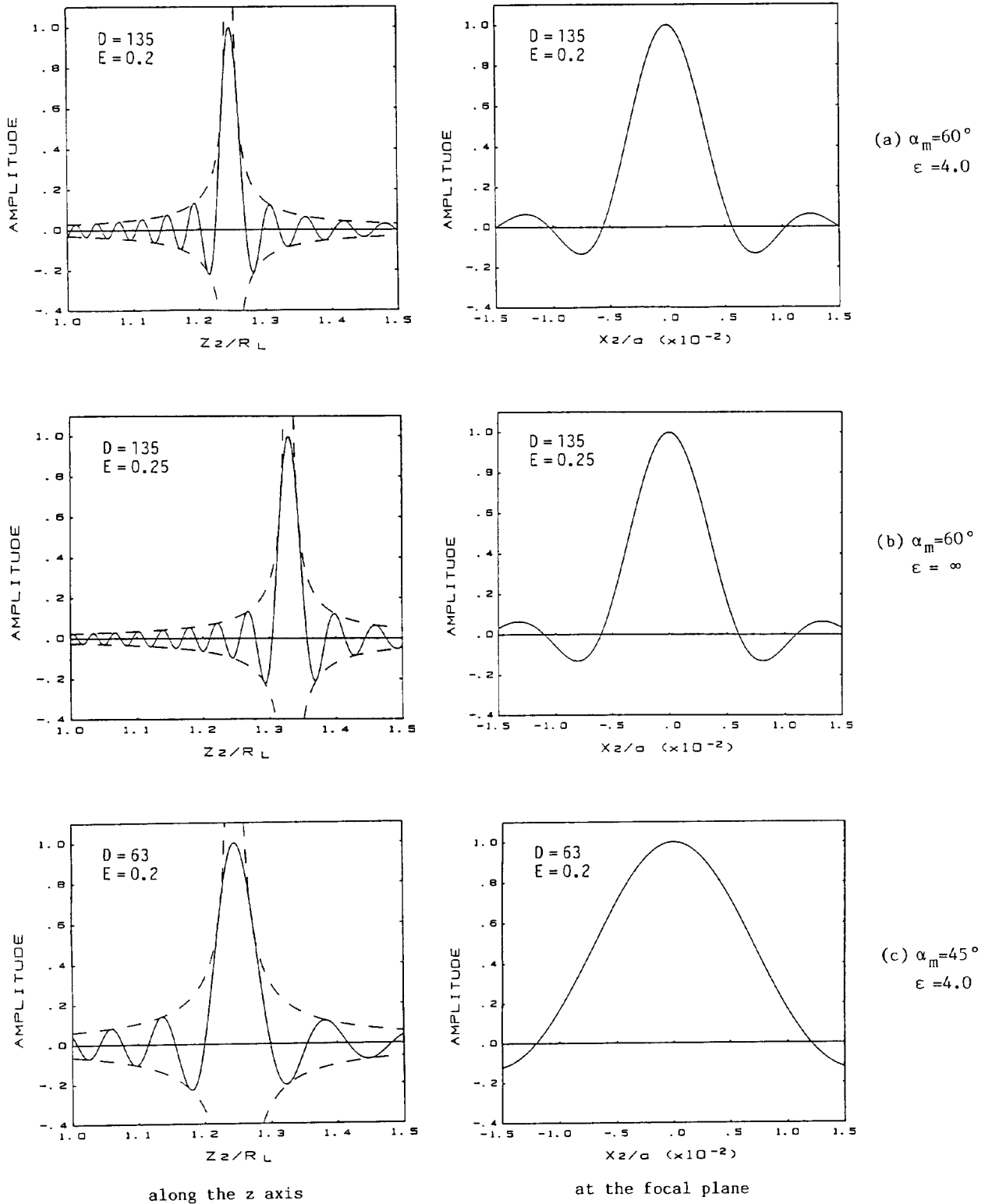
along the z axis · · · at the focal plane

Fig. 3 Acoustic field distributions along the z axis and
at the focal plane calculated for fused quartz rod
($f=200MHz$, $R_L=1.0$ mm).

Next, let us consider the relationship in the focusing characteristics among the three focusing devices. Figure 4 shows the focusing characteristics as a function of the normalized eccentricity ε in a case of D=135 having the following parameters: the acoustic frequency of 200 MHz, the radius of curvature of the concave aperture of 1.0 mm, and the maximum opening angle of 60°. Figures 4(a) and 4(b) are for fused quartz and sapphire, respectively. Here, the focal length, the beam width (half of relative amplitude), the position of the sidelobe, and the amplitude of the sidelobe are considered as the quantities associated with the focusing characteristics, which can be obtained theoretically from Eq. (8) for a large value of D. The scale for the beam width and for the position of the sidelobe is in terms of $V=x_2/a$. The scale of the

focal length is in terms of $W=z_2/R_L$. In Fig. 4, the solid lines and the dashed-and-dotted lines represent the results calculated by the present theory, while the the closed circles and the opened circles represent the corresponding results obtained by the direct calculation under diffraction theory taking into consideration the diffraction of the acoustic field in the solid rod and the transmittance for acoustic waves across the boundary between the solid rod and the liquid. The present theory shows that, in the range of the normalized eccentricity ε from 0 to 5 for fused quartz and from 0 to 2 for sapphire, the beam width, the focal length, and the position of the sidelobe increase rapidly with increasing of ε. In the range of larger normalized eccentricity ε, those values reach to constant. It can be seen that the solid rods with high
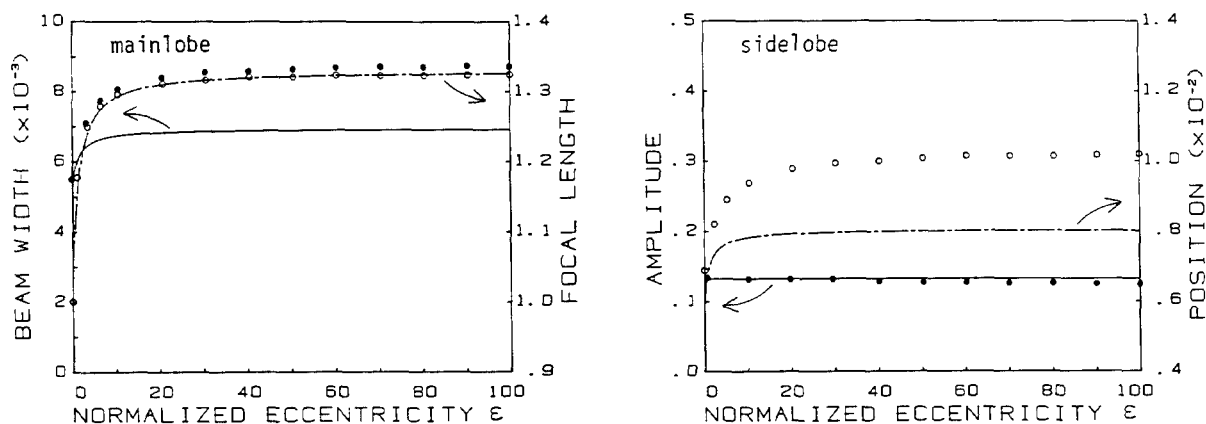
(a) fused quartz
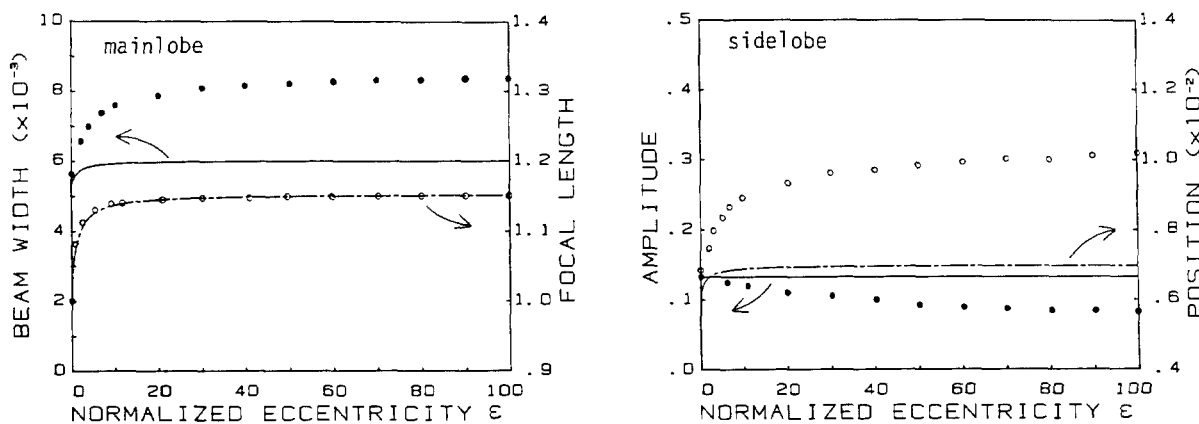
(b) sapphire

Fig. 4 Focusing characteristics as a function of normalized eccentricity ε.
The two ultimate limits of the normalized eccentricity, ε =0 and ε = ∞,
correspond to a concave transducer and an acoustic lens, respectively.
The solid lines (——) and dashed-and-dotted lines (—·—) represent
the results obtained by the present theory, while the closed circles
(•) and opened circles (o) represent the corresponding results
obtained by the direct calculation (f; 200 MHz, R_L; 1.0 mm, α_m; 60 °).

velocity such as sapphire are required to design an excellent focusing performance at a high normalized eccentricity ε. It can be also seen that with the off-centric concave transducer an almost same excellent focusing performance is expected as that of sapphire rod by designing the normalized eccentricity ε at a small value, even for rod materials such as fused quartz with relatively small velocity. The results obtained by the present approach give a similar tendency to those attained by the direct calculation, so that this analysis will be preferably accepted to speculate the focusing performance of the devices without the complicated calculation on diffraction theory. The reasonable results are naturally obtained that the excellent focusing characteristics are expected for the use in acoustic microscopes with increasing of D and/or decreasing of E.

From the above analysis, two parameters of D and E may be called as "field design parameters", because the effect of the various parameters (such as acoustic frequency, materials used for solid rod and liquid, radius of curvature of concave aperture, and opening angle of the concave aperture) on the focused field distributions can be easily understood by these parameters without the complicated numerical calculation.

4. CONCLUSION

A unified analysis of the focusing devices in acoustic microscopy was derived. It was carried out by combining the wavefront optics approach and the wave optics approach. First, the field distribution radiated from the concave surface was derived by the wavefront optics approach. Then, the field distribution formed by this concave aperture was derived using the Lommel's approximation method. It has been shown that the focused field distribution of such devices can be systematically determined by introducing the two parameters $D = a^2/R_L\lambda_L$ (a is the radius of concave surface, R_L is the radius of curvature of the concave aperture, and λ_L is the wavelength in the liquid) and $E = (k_S/k_L)(\varepsilon/(1+\varepsilon))$ (k_S and k_L is the propagation constants in the solid rod and in the liquid, respectively, and ε is the normalized eccentricity). Both results of the focusing characteristics obtained by the present approach and by the direct calculation gave a similar tendency to reveal the significant advantages of the present study for understanding the characteristics of the focusing devices. We conclude that the principal performance of the focusing devices in acoustic microscopy can be systematically understood by using the acoustic field design parameters D and E proposed in this paper.

Recently, it is required to design the acoustic beams with large focusing depth and the convergence in some degree for investigating the internal inspection of the solid material as well as the biological specimen, so that the present analysis can be expected to be applied for the design purpose of such focusing devices.

REFERENCES

[1] R.A.Lemon and C.F.Quate, IEEE Ultrason. Symp., pp.18-20(1973).
[2] N.Chubachi, J.Kushibiki, T.Sannomiya, and Y.Iyama,IEEE Ultrason.Symp.,pp.415-418(1979).
[3] N.Chubachi, J.Kushibiki, K.Nakanishi, and Y.Sugawara,in Proc. Acoust. Soc. Japan, pp.631-632, Mar.(1984).
[4] A.Pettinen and Luukkala, J. Phys. D: Appl. Phys. 9, pp.1927-1936(1976).
[5] A.Atalar, J. Appl. Phys. 49(10), Oct. pp.5130-5139(1978).
[6] H.K.Wickramasinghe, J. Appl. Phys. 50(2), Feb. pp.664-672(1979).
[7] E.Bridoux, B.Nongaillard, J.M.Rouvean, C.Bruneel, G.Thomin, and R.Torguet, J. Appl. Phys. 49(2), pp.574-579(1978).
[8] E.Cavanagh and B.D.Cook, J. Acoust. Soc. Am. 69(2), pp.345-351(1981).
[9] O'Neil, J.Acoust.Soc.Am.21,pp.516-526.(1949).
[10] T.Torikai, Report of the Institute of Industrial Sience, University of Tokyo, 25,Mar.(1976).
[11] Y.Sugawara, J.Kushibiki, and N.Chubachi, in Proc. Acoust. Soc. Japan, pp.597-598, Mar.(1985).
[12] N.Chubachi, J.Kushibiki, and Y.Sugawara, Jpn. J. Appl. Phys. 12(1985), Suppl. 25-1, pp.203-205(1985).
[13] E.Lommel, Abd. der K Bayer, Akad.der Wissen, 15, p.233(1886).